World Journal of Gastrointestinal Oncology

Submit a Manuscript: https://www.f6publishing.com

World J Gastrointest Oncol 2024 October 15; 16(10): 4232-4243

DOI: 10.4251/wjgo.v16.i10.4232

ISSN 1948-5204 (online)

ORIGINAL ARTICLE

Basic Study

Intratumoural microorganism can affect the progression of hepatocellular carcinoma

Bao-Qun Liu, Yi Bai, Da-Peng Chen, Ya-Min Zhang, Tian-Ze Wang, Jing-Rui Chen, Xiang-Yu Liu, Bin Zheng, Zi-Lin Cui

Specialty type: Oncology

Provenance and peer review: Unsolicited article; Externally peer reviewed.

Peer-review model: Single blind

Peer-review report's classification
Scientific Quality: Grade C
Novelty: Grade B
Creativity or Innovation: Grade B
Scientific Significance: Grade C

P-Reviewer: Giacomelli L

Received: June 15, 2024
Revised: July 29, 2024
Accepted: August 12, 2024
Published online: October 15, 2024
Processing time: 102 Days and 18.9 Hours

Bao-Qun Liu, Da-Peng Chen, Jing-Rui Chen, First Central Clinical College, Tianjin Medical University, Tianjin 300070, China

Yi Bai, Ya-Min Zhang, Zi-Lin Cui, Department of Hepatobiliary Surgery, Tianjin First Central Hospital, School of Medicine, Nankai University, Tianjin 300192, China

Tian-Ze Wang, Xiang-Yu Liu, Tianjin First Central Hospital Clinic Institute, School of Medicine, Nankai University, Tianjin 300192, China

Bin Zheng, School of Medicine, Tianjin University, Tianjin 300072, China

Co-first authors: Bao-Qun Liu and Yi Bai.

Co-corresponding authors: Bin Zheng and Zi-Lin Cui.

Corresponding author: Zi-Lin Cui, Doctor, Chief Doctor, Surgeon, Department of Hepatobiliary Surgery, Tianjin First Central Hospital, School of Medicine, Nankai University, No. 24 Fukang Road, Nankai District, Tianjin 300192, China. 13602184643@163.com

Abstract

BACKGROUND

Several recent studies have confirmed that intratumoural microorganisms can affect the occurrence and development of hepatocellular carcinoma (HCC); however, their role in tumor progression remains unclear. Hence, there is a need for further research on the role of intratumoural microorganisms in HCC.

AIM

To investigate the changes in intratumoural microorganisms in HCC and the effect of *Propionibacterium* on HCC progression.

METHODS

HCC and normal liver tissue specimens were subjected to fluorescence *in situ* hybridization (FISH). After performing 16S rRNA sequencing on HCC and peritumoral tissues to analyze the differences between the two groups. *Propionibacterium* was cocultured with HCC cells *in vitro*. Changes in cell proliferation and migration capacity were evaluated. The expression of NF-κB pathway related proteins in tumor cells was compared. The orthotopic liver implantation model

and the subcutaneous xenograft model were constructed. liver tissues and subcutaneous tumors were collected 2 weeks later.

RESULTS

FISH demonstrated the presence of microorganisms in HCC and normal liver tissues. 16S rRNA sequencing revealed an abundance of *Lysobacter*, *Lachnospiraceae*, *Pseudomonas*, and *Lactobacillus* in HCC tissues. The distribution and abundance of *Propionibacterium* showed differences between HCC and peritumoral tissues ($P < 0.05$). *In vitro* studies demonstrated that *Propionibacterium* and its metabolite propionic acid (PA) inhibited the proliferation and migration of HCC cells ($P < 0.05$). The expression of the proteins in NF-κB signaling pathway also decreased in HCC cells ($P < 0.05$).

CONCLUSION

Microorganisms in HCC and normal liver tissues displayed significant disparities. The PA-producing bacterium *Propionibacterium* in HCC exerts an effect on the NF-κB pathway, thereby affecting the biological behavior of HCC.

Key Words: Hepatocellular carcinoma; Intratumoural microbiome; 16S rRNA sequencing; *Propionibacterium*

Core Tip: Significant changes were detected in hepatocellular carcinoma (HCC) microbiomes. *Propionibacterium* can alter the proliferation and migration of HCC cells, mediate the NF-κB signaling pathway, and impact HCC progression. This study provides useful insights to investigate the microbiome composition of HCC and inhibit its progression.

Citation: Liu BQ, Bai Y, Chen DP, Zhang YM, Wang TZ, Chen JR, Liu XY, Zheng B, Cui ZL. Intratumoural microorganism can affect the progression of hepatocellular carcinoma. *World J Gastrointest Oncol* 2024; 16(10): 4232-4243
URL: https://www.wjgnet.com/1948-5204/full/v16/i10/4232.htm
DOI: https://dx.doi.org/10.4251/wjgo.v16.i10.4232

INTRODUCTION

Liver cancer is the third leading cause of cancer-related deaths worldwide, with its incidence being increasing annually[1,2]. Statistically, 75%-85% of primary liver cancers are classified as hepatocellular carcinoma (HCC) in pathology, and the number of patients in China accounts for > 50% of global HCC cases[1,3]. HCC primarily occurs in patients with liver cirrhosis caused by hepatitis virus infection, fatty liver disease and alcohol-related cirrhosis[4]. Despite remarkable progress in HCC treatment over the past few decades, there is limited knowledge regarding the exact molecular mechanism.

Exploring the role of intratumoral microbes in the tumor has been a prominent research direction over the past decade. Intratumoural microorganisms have been detected in various solid tumors, including HCC[5]. Research on tumor-related microorganisms has been facilitated by various technological advancements that have overcome certain barriers. For instance, the TCGA database was used by Poore *et al*[6] to delineate distinct microbial profiles associated with different cancer types. 16S rRNA sequencing also revealed distinct microbial compositions between tumors and their adjacent tissues[7]. Furthermore, Ghaddar *et al*[8] developed single-cell analysis of host-microbiome interactions for investigating a cohort of human pancreatic cancer, and discovered that the tumor-infiltrating lymphocytes and T cells derived from infected tissues exhibited remarkable similarities.

Recent research has successfully identified and localized these microbes within cancer and immune cells, and has demonstrated advancements in detection technologies from a different perspective[9]. For instance, Ma *et al*[9] showed that the presence of the butyrate-producing bacterium *Roseburia* in lung cancer resulted in the polarization of M2 macrophages, causing an increase in H19 expression within tumor cells. This mechanism ultimately facilitated lung cancer. Intratumoral microorganisms may serve as biomarkers for early diagnosis and prognostic analysis in the future, while also exerting an impact on the regulation of the host immune system and finding applications in clinical therapy [10].

Intratumoral microbes are known to be associated with tumor progression, emphasizing their potential for future applications in the diagnosis and treatment of tumors. Nonetheless, there is still limited research on the tumor microbiome of HCC. Therefore, this study was conducted to analyze the changes in the microbiome of HCC tumor tissues to explore the specific mechanism of action of the flora in HCC.

MATERIALS AND METHODS

Patients and tissue samples

This study was approved by the ethics review board of Tianjin First Central Hospital (Tianjin, China). A total of 10 HCC tissue specimens, including both HCC and adjacent noncancerous tissues, were used for 16S rRNA sequencing. The inclusion criteria were as follows: Pathological diagnosis of confirmed primary HCC, solitary HCC, now previous treatment for HCC, and detailed clinical histories. All clinical samples were collected after obtaining informed consent from patients.

All samples were collected under sterile conditions in an operating room, after which the specimens were promptly frozen in a liquid nitrogen tank and then stored at -80 °C.

Fluorescence in situ hybridization

The cyanine 3-labeled fluorescence *in situ* hybridization (FISH) probe EUB338 (5′-GCT GCC TCC CGT AGG AGT-3′) could specifically label bacterial 16S RNA. The probe and the frozen tissue slides that had been digested were subjected to denaturation at 75 °C for 8 min. The denatured probe was immediately transferred to ice and incubated for 5 minutes. The slides were dehydrated using ethanol gradients of 70%, 80%, 90%, and 100% followed by natural air-drying. After adding the probe, the slides were transferred to a dark environment at 37 °C for overnight hybridization. Cell nuclei were stained with DAPI on the second day. Then, the stained slides were observed under a fluorescence microscope (Nikon A1, Japan) after adding fluorescent antifade reagents (Beyotime Biotechnology, China).

16S rRNA sequencing and data analysis

16S rRNA sequencing was performed by Biomarker Technologies Co (Beijing, China). DNA was extracted from HCC and peritumoral tissue samples, followed by amplification of the V3-V4 region of the bacterial 16S rRNA gene. Using lima (v 1.7.0), circular consensus sequencing (CCS) sequence data were identified by the barcode, and raw-CCS sequence data were obtained. After identifying the primer sequence and filtering the length, an effective CCS sequence was obtained using UCHIME (v 4.2) to identify and remove the chimeric sequence. At a 97.0% similarity level, Usearch was used to cluster the data and obtain operational classification units (OTUs). Using SILVA as a reference database and the naive Bayes classifier combined with the comparison method, the feature sequences were annotated. The results of species annotation were visualized using KRONA (v 2.6). The alpha diversity of the sample was calculated using QIIME2 (2020.6) and expressed as Shannon indices. Based on the distance matrix obtained from the beta diversity analysis (QIIME), the results of principal coordinates analysis were plotted using the R package. The linear discriminant analysis effect size method was used to detect statistically significant differences.

Cell culture and reagents

The HCC cell lines (HUH-7 and HCC-LM3) were stored in our laboratory. All HCC cells were cultured in Dulbecco's modified Eagle's medium containing 10% fetal bovine serum (FBS). Propionic acid (PA; jskchem, 79-09-4) was used in the PA-related experiments. *Propionibacterium acidipropionici* (BNCC134322), purchased from Beijing Biao Biotechnology Company, was cultured in FTM under anaerobic conditions at 37 °C.

Cell proliferation assay

After coculture with *Propionibacterium* and PA for 24 hours, HUH-7 and HCC-LM3 cells were seeded into 96-well plates at a density of 2×10^4/mL in each well. Next, 100 μl of cell medium and 10 μl of CCK-8 reagent (Beyotime, C0037) were added to each well, after which the cells were incubated at 37 °C for 3 hours. Absorbance was measured at 450 nm using a microplate reader (Biorad, Model 680).

Wound healing assay

HUH-7 and HCC-LM3 cells were seeded into 12-well plates. When the cells reached 100% confluence, the cell monolayer was gently scratched with the tip of a 10-μl pipette. The cells were washed twice with phosphate buffer saline (PBS), and the remaining cells were cultured in a medium without FBS. Images of the scratch areas were captured at 0, 12, and 24 hours. Experiments for each group were conducted in triplicates.

Transwell assay

The migratory capacity of HCC cells was evaluated using a Transwell (8-mm pore size; Corning Inc.) assay *in vitro*. Cells (5×10^4) were inoculated into the upper chamber containing 600 μl of serum-free medium, and medium supplemented with 10% FBS was added to the lower chamber as a chemoattractant. After incubation for 24 hours, unmigrated cells on the upper surface of the membrane were removed using a cotton swab, and migrated cells were fixed with formaldehyde for 30 minurtes and stained with 0.5% crystal violet for 40 minutes. The migrated cells were quantified in five randomly selected fields under a microscope.

Western blot analysis

HUH-7 and HCC-LM3 cells were incubated with *Propionibacterium* and PA (15 mmol/L) for 72 hours in 6-well plates, followed by washing three times with cold PBS. After lysing with Cell Lysis Buffer (Beyotime Biotechnology, China) for 30 minutes on ice, the cells were centrifuged at 12000 rpm for 10 minutes at 4 °C. The resulting supernatant was collected and quantified using a BCA protein assay kit (Beyotime Biotechnology, China), followed by the addition of 5 × sodium

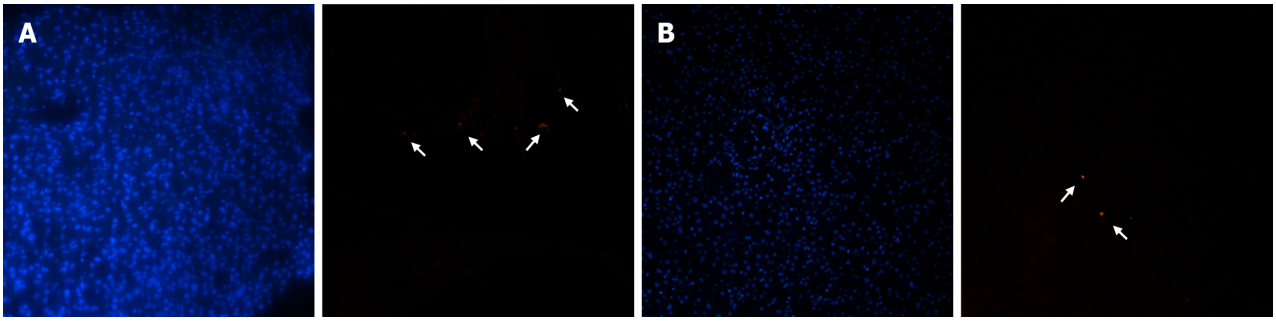

Figure 1 Microbiomes presented in hepatocellular carcinoma tissue. Fluorescence *in situ* hybridization (FISH) was performed on slides of human hepatocellular carcinoma (HCC) and normal liver tissue. A: Fluorescence microscopy was used to analyze FISH signals in HCC; B: FISH signal in normal liver tissue. The image on the left depicts DAPI staining, while the image on the right illustrates EUB338 probe staining.

dodecyl sulfate (SDS) and boiling for 5 min. Equal amounts of protein were added to a prepared 10% SDS-PAGE gel for electrophoretic separation. The membranes were incubated overnight with cleaved specific primary antibodies including NF-κB p65 (1: 100080979-1-RR) and p- NF-κB p65 (1: 100082335-1-RR) at 4 °C. After washing with 1 × TBST for 10 minutes, the membranes were incubated with anti-mouse secondary antibodies for 1 h. Results were evaluated by exposure to the NcmECL Ultra ECL reagent (NCM BIO.CTD, China).

Animal experiments

A total of 16 C57 female mice (SPF level, aged 6-8 weeks, purchased from Huafukang, China, were allocated to two models: The orthotopic liver implantation model and the subcutaneous xenograft model. Each model had eight mice, and the models were subsequently divided into experimental and control groups. Mice in the control group were injected with 1.5 × 10^6 HEP1-6 cells alone, whereas mice in the experimental groups were injected with a combination of an identical quantity of HEP1-6 cells and *Propionibacterium*. In the orthotopic liver implantation model, the mice were adequately anesthetized and securely immobilized in a supine position, and cells were injected into the left lobe of the liver after laparotomy. In the subcutaneous xenograft model, the mice were anesthetized and immobilized in the left lateral position, and cells were injected 1 cm below the right shoulder of each mouse. The mice were fed on a conventional mouse diet and water. At 2 weeks after the injection, the mice were euthanized. The length and width of each tumor were measured using a digital caliper, and the tumor volume was calculated using the following formula: Tumor volume = (width^2 × length)/2. All animal experiments were approved by the Animal Ethics Committee of Tianjin First Central Hospital.

Statistical analysis

All statistical analyses were conducted using, GraphPad Prism 9.5 (GraphPad Software, United States) and SPSS 19.0 (SPSS, United States). Variations across experimental groups were evaluated using either the Student's *t*-test or one-way ANOVA. A P value of < 0.05 indicated statistically significant differences.

RESULTS

Microbiomes in HCC tissues

We utilized the EUB338 probe was used for FISH assays on clinically obtained tumor samples to confirm the presence of microbiome in HCC tissues (Figure 1A). The heterogeneity of the microbiome between the tumor and adjacent tissues was further investigated by performing FISH on peritumoral tissue samples (Figure 1B). FISH signals were observed in both tumor and peritumoral tissues, with remarkably higher abundance and distribution in HCC samples. In addition, more FISH signals were observed in HCC cells than in hepatobiliary cells.

Heterogeneous microbiome in HCC and peritumoral tissues

High-throughput 16S rRNA gene sequencing techniques are widely used for microbiological analysis, which enable the determination of microbiome composition and abundance in various tissues. In this study, the sequencing cohort contained 10 HCC and paired adjacent tissue samples, which were obtained from the surgical specimens of patients with HCC. Sequencing yielded 585,428 high-quality valid readings, clustering into 4994 TUs. *Lysobacter*, *Lachnospiraceae*, *Pseudomonas*, and *Lactobacillus* were highly abundant at the genus level, including in the HCC and peritumoral groups (Figure 2A).

The disparities in bacterial composition between the HCC and peritumoral groups were further investigated, which revealed that 2112 OTUs were shared between the two groups in the Venn diagram (Figure 2B). The α diversity indicated the species richness and diversity of individual samples, and the Shannon index showed a significant disparity between the HCC and peritumoral groups (7.93 ± 0.65 *vs* 7.33 ± 0.26, P < 0.05, Figure 2C). The analysis of NMDS pertaining to β diversity revealed significant differences among the groups (P < 0.05, Figure 2D). Data analysis revealed that the abundance of *Propionibacterium* was significantly higher in the HCC group than in the peritumoral group (0.00036 *vs*

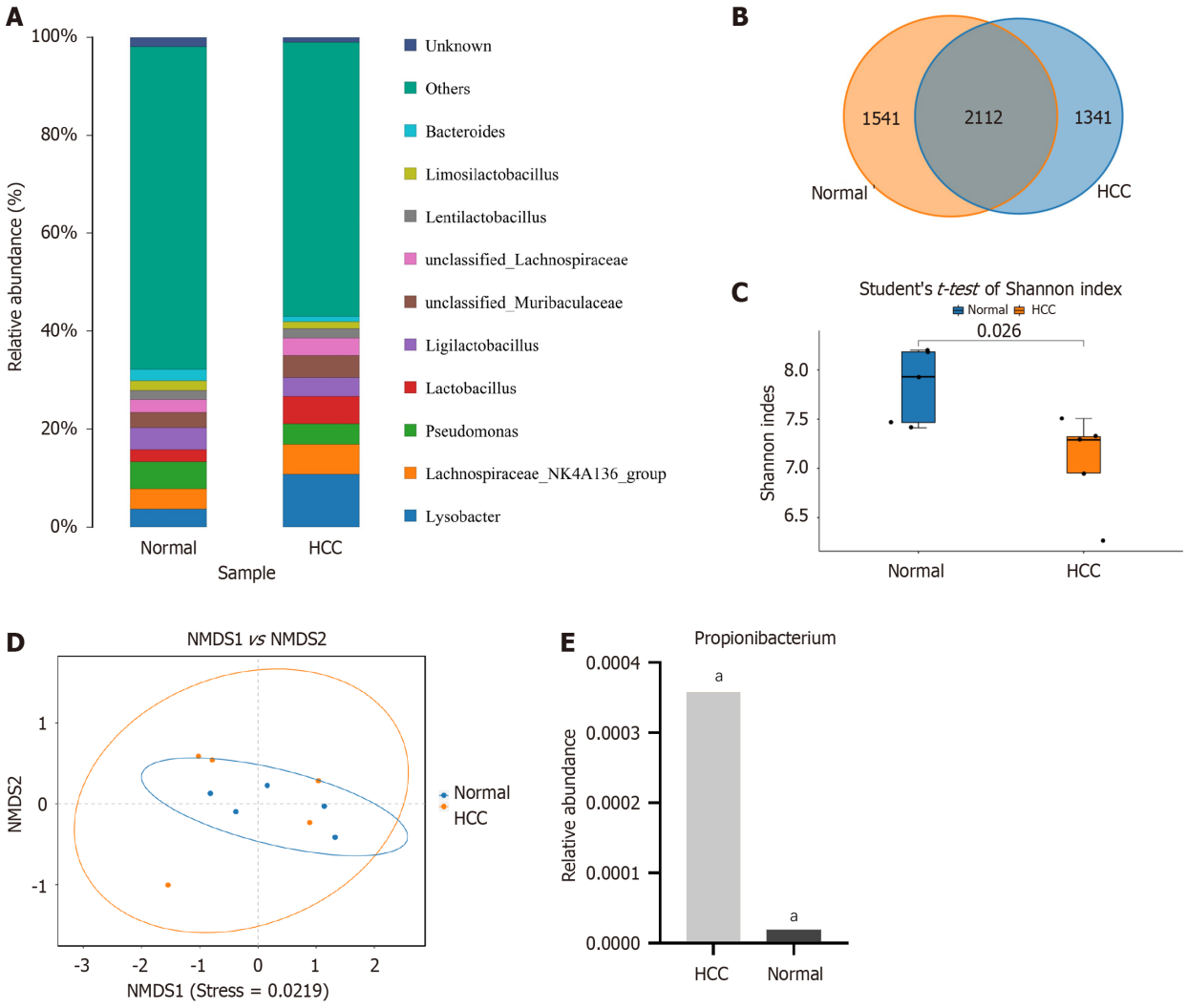

Figure 2 Heterogeneous microbiome in hepatocellular carcinoma and peritumoral tissue. A: The abundance of microbiomes in hepatocellular carcinoma (HCC) and peritumoral tissues ranked among the top 10 at the generic level; B: Venn diagram of operational classification units composition in HCC and peritumoral tissues; C: Shannon index of response alpha diversity; D: The β diversity exhibited substantial disparities between the HCC and peritumoral groups; E: Relative content of *Propionibacterium* in HCC and peritumoral tissues. ($^{a}P < 0.001$). HCC: Hepatocellular carcinoma.

0.00002, $P < 0.01$, Figure 2E).

Propionibacterium inhibited the proliferation and migration of HCC cells

The sequencing results revealed differences in the abundance and distribution of *Propionibacterium* in HCC and peritumoral tissues. Our aim was to determine whether *Propionibacterium* contributes to tumor progression. To confirm the role of *Propionibacterium* in the development of HCC, we first selected the commonly used HUH-7 and HCC-LM3 cells for coculture with *Propionibacterium* and its supernatant. The supernatant was obtained by harvesting the liquid culture medium of *Propionibacterium*, followed by high-speed centrifugation and filtration. The CCK-8 assay indicated that *Propionibacterium* and its supernatant inhibited the proliferation of HUH-7 cells ($P < 0.001$, Figure 3A). The wound healing assay revealed significantly impaired migratory capacity of HUH-7 and HCC-LM3 cells at 24 h ($P < 0.001$, Figure 3B-E). The number of HCC cells in the *Propionibacterium* groups that migrated through the Transwell polycarbonate filter was remarkedly lower than that of cells in the control group ($P < 0.01$, Figure 3F-H), which was similar to the tendency observed in the supernatant group in HUH-7 and HCC-LM3 cells ($P < 0.01$, Figure 3F and H). These findings indicated showed that coculture with *Propionibacterium* and its supernatant significantly reduced the migration ability of HCC cells compared with that in the control group.

PA played an inhibitory role as a metabolite of Propionibacterium

The above described cellular experimental findings substantiated the inhibitory effects of *Propionibacterium* on the proliferation and migration of HCC cells, with similar results observed in the supernatant group. The metabolite PA, derived from the standard strain of *Propionibacterium*, was initially cocultured with HCC cells. To select the appropriate PA concentration, six groups were set respectively, viz., 4, 8, 16, 25, and 50 mM. We observed that with an increase in PA concentration, the viability of HCC cells decreased ($P < 0.001$, Figure 4A). Therefore, we selected 10 mM PA concentration

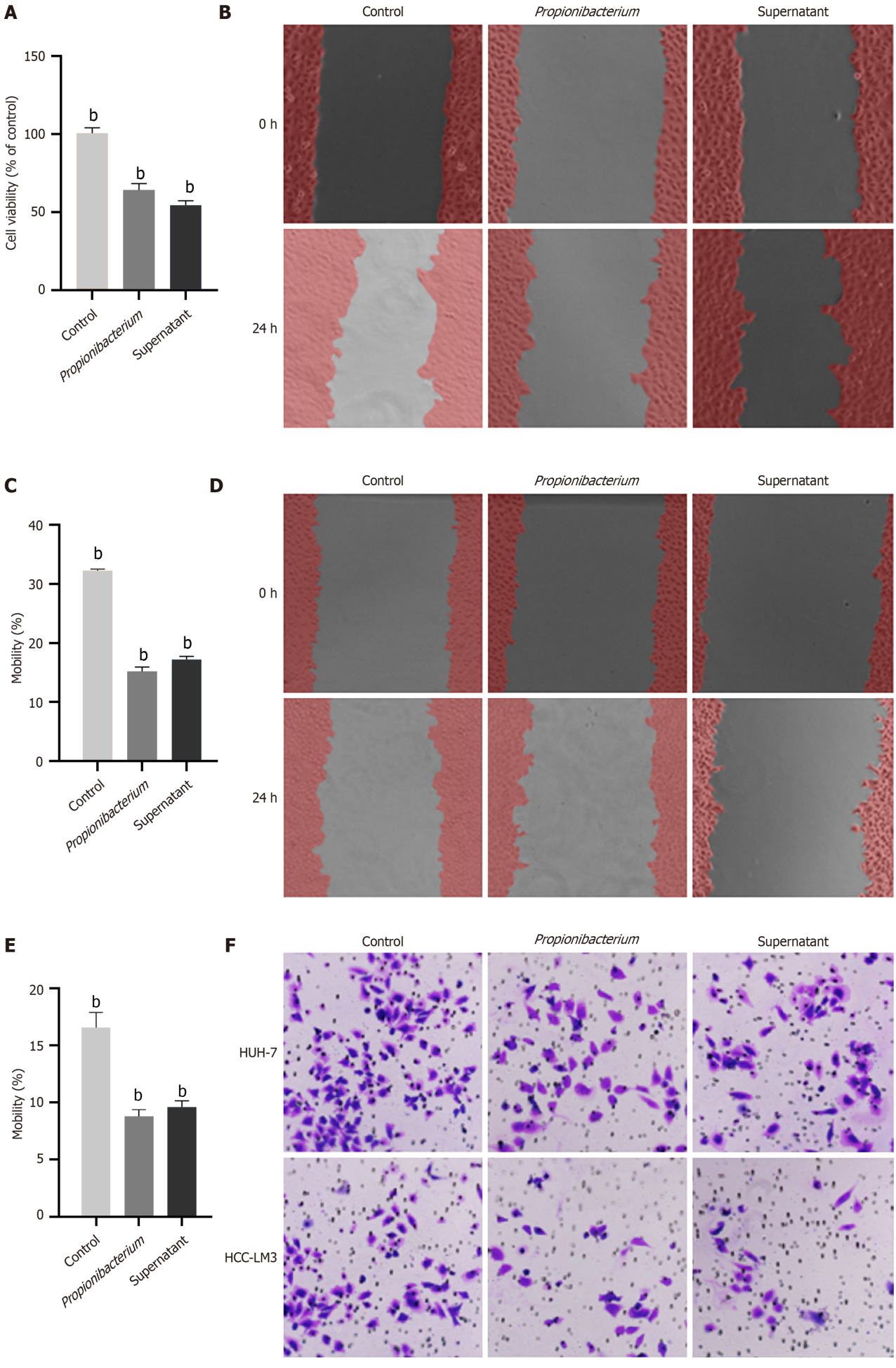
A
Cell viability (% of control)
150
100
50
0
b
b
b
Control
Propionibacterium
Supernatant
B
Control
Propionibacterium
Supernatant
0 h
24 h
C
Mobility (%)
40
30
20
10
0
b
b
b
Control
Propionibacterium
Supernatant
D
Control
Propionibacterium
Supernatant
0 h
24 h
E
Mobility (%)
20
15
10
5
0
b
b
b
Control
Propionibacterium
Supernatant
F
Control
Propionibacterium
Supernatant
HUH-7
HCC-LM3

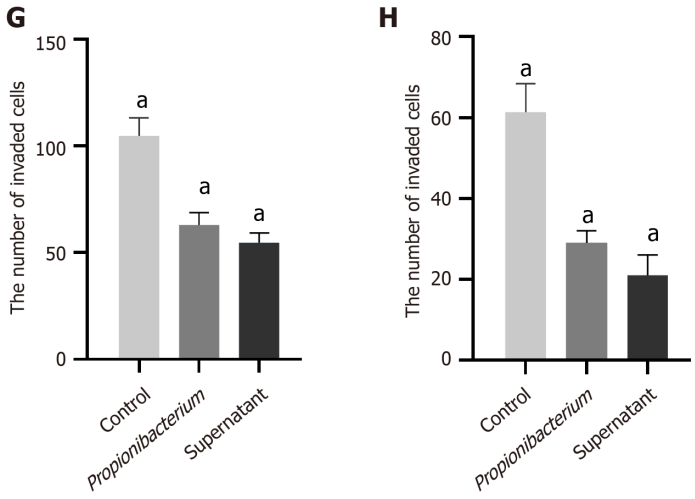

Figure 3 *Propionibacterium* inhibited the proliferation and migration of hepatocellular carcinoma cells. A: Cell viability was measured through CCK-8 assay. HUH-7 cells were exposed to *Propionibacterium* and its supernatant; B: The migration of HUH-7 cells in control, *Propionibacterium* and supernatant groups was evaluated by wound healing assay; C: Changes in mobility of HUH-7 cells; D: Results of 24 hours wound healing assay on hepatocellular carcinoma (HCC)-LM3 cells; E: Changes in migration rate of HCC-LM3 cells; F: Transwell assay of HUH-7 and HCC-LM3 cells. The migrating cells were observed using a 40 × microscope; G: The quantity of migrated HUH-7 cells; H: The quantity of migrated HCC-LM3 cells. $^{a}P < 0.0001$, $^{b}P < 0.001$.

was selected for subsequent experiments.

The effect of PA on cellular migration was evaluated using a scratch assay. We observed that a decrease in the mobility of HUH-7 and HCC-LM3 cells to different degrees, with that of HCC-LM3 cells being more significantly inhibited ($P < 0.001$, Figure 4B-E). The Transwell assay further confirmed that PA inhibited the migration ($P < 0.001$, Figure 4F-H). Thus, the effect of PA on the proliferation and migration of HUH-7 and HCC-LM3 cells was confirmed using *in vitro* experiments.

Propionibacterium and PA inhibited the NF-κB pathway

The effect of *Propionibacterium* and its metabolite PA on the biological behavior of HCC cells was confirmed in the above described experiments. We next investigated the precise signaling pathways to discern the underlying mechanisms. NF-κB functions as a transcription factor involved in various physiological and pathological processes. The involvement of P65, a member of the NF-κB family, in the transcription of target genes within the classical pathway has been established. Signal-induced phosphorylation of IκB molecules is a fundamental step in canonical NF-κB activation[11]. Phosphorylated IκBα undergoes degradation through ubiquitination in response to the stimulus signal, resulting in the translocation of the NF-κB p65/p50 dimer from the cytoplasm to the nucleus by dissociation from IκB. This process subsequently facilitates the transcriptional activation of target genes[12].

In this study, we investigated the role of *Propionibacterium* and its metabolite PA in the NF-κB signaling pathway was investigated using western blotting and immunohistochemistry assays. Western blotting was conducted to examine the expression of phosphorylated and unphosphorylated NF-κB p65 (p-NF-κB p65/NF-κB p65). The expression of p-NF-κB p65 decreased significantly after coculturing with *Propionibacterium* and PA (Figure 5A). The expression of NF-κB p65 in HCC tissues significantly decreased compared with that in normal liver tissues in quantitative results ($P < 0.001$, Figure 5B and C).

Propionibacterium and PA repressed in vivo HCC tumorigenesis

Mouse HCC HEP1-6 cells were used for orthotopic liver implantation and subcutaneous xenograft of 6-week-old C57 mice. Tumor formation was observed 2 weeks after the subcutaneous injection of HEP1-6 cells into mice (Figure 6A). Subcutaneous tumors were removed after sacrificing the mice, and we observed the tumors in the Propionibacterium group were reduced in size upon visual inspection (Figure 6B). Statistical results also revealed a decrease in tumor size in the Propionibacterium group compared with that in the control group (305.63 ± 26.67 *vs* 61.50 ± 5.64, $P < 0.05$, Figure 6C). In the orthotopic liver implantation model, the control group exhibited greater tumor volume and more extensive invasion (Figure 6D). After dissection and analysis, tumors in the Propionibacterium group exhibited statistically significant reductions in volume (186.25 ± 16.35 *vs* 64.63 ± 4.23, $P < 0.05$, Figure 6E).

DISCUSSION

The third generation complete 16S gene sequencing technology has become a commonly used approach and has promoted the accurate identification of bacterial species[12]. In this study, the sequencing data revealed significant heterogeneity in microbial composition among the different samples within the HCC group. The HCC samples exhibited a significantly high abundance of *Lysobacter*, *Lachnospiraceae*, *Pseudomonas*, and *Lactobacillus*. However, the contribution of

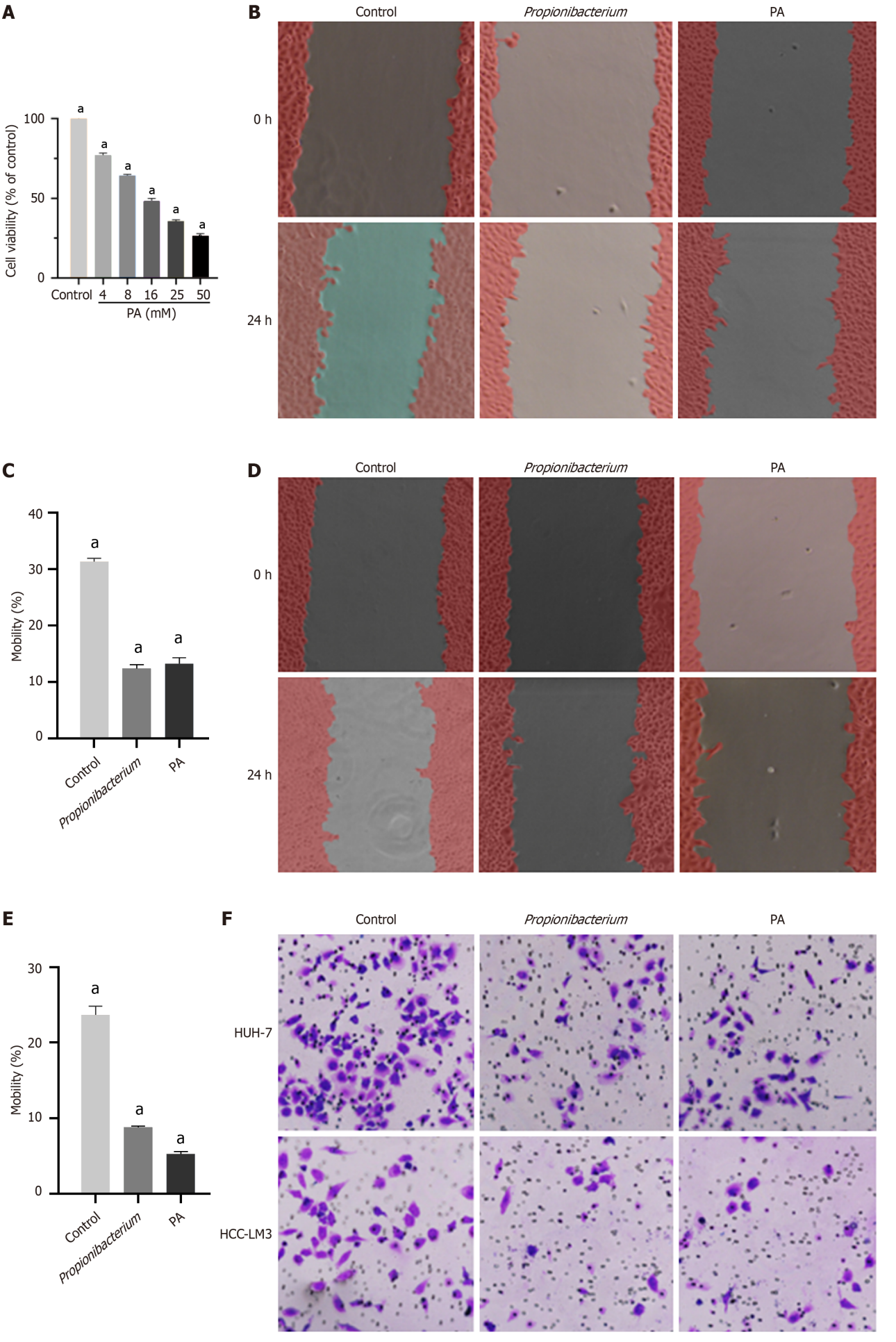
A
Cell viability (% of control)
100
50
0
a
a
a
a
a
a
Control
4
8
16
25
50
PA (mM)
B
Control
Propionibacterium
PA
0 h
24 h
C
Mobility (%)
40
30
20
10
0
a
a
a
Control
Propionibacterium
PA
D
Control
Propionibacterium
PA
0 h
24 h
E
Mobility (%)
30
20
10
0
a
a
a
Control
Propionibacterium
PA
F
Control
Propionibacterium
PA
HUH-7
HCC-LM3

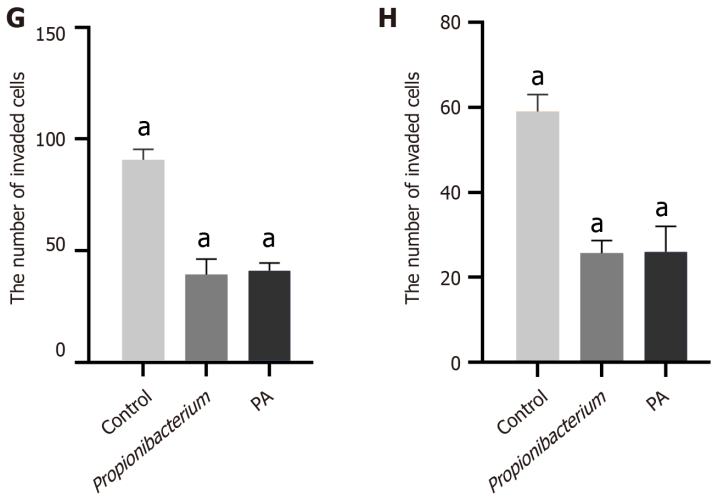

Figure 4 Propionic acid played an inhibitory role as a metabolite of *Propionibacterium*. A: Effects of different concentrations of propionic acid (PA) on the cell viability of HUH-7 cells; B: Wound healing assay results of HUH7 cells in control, *Propionibacterium* and PA group; C: Changes in mobility of HUH-7 cells; D: Results of wound healing assay on hepatocellular carcinoma (HCC)-LM3 cells; E: The mobility of HCC-LM3 cells in *Propionibacterium* and PA groups decreased significantly; F: Transwell assay results of HUH7 and HCC-LM3 cells; G: The quantity of migrated HUH-7 cells; H: The quantity of migrated HCC-LM3 cells. $^{a}P <$ 0.0001. PA: Propionic acid.

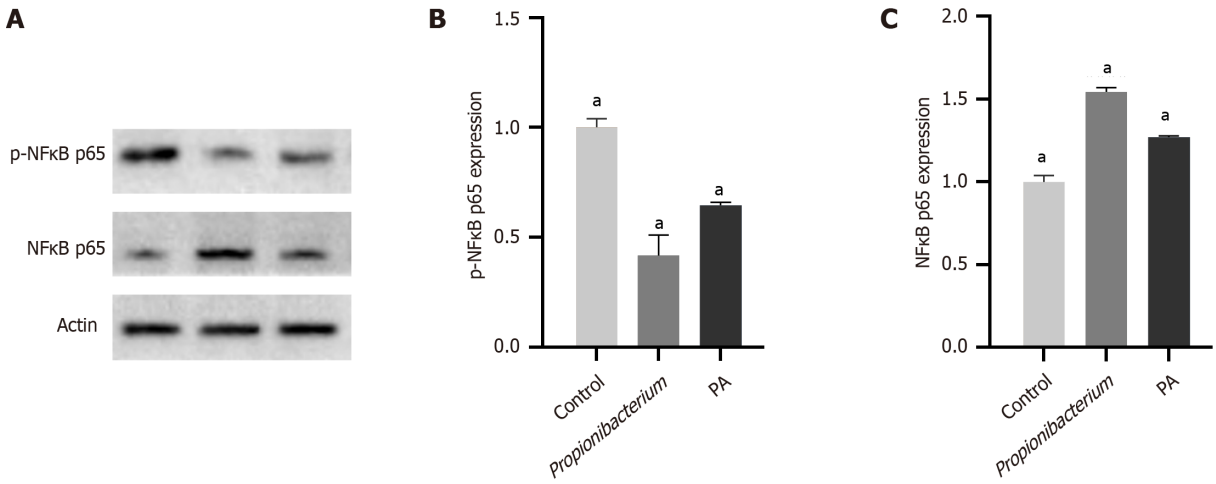

Figure 5 *Propionibacterium* and propionic acid inhibited the NF-κB pathway. A: Western blot was performed after coculture of *Propionibacterium* and propionic acid (PA) with HUH-7 cells; B: Relative expression level of p-NF-κB p65. The expression of p-NF-κB p65 was significantly decreased in *Propionibacterium* and PA groups; C: Relative expression level of NF-κB p65. $^{a}P <$ 0.0001. PA: Propionic acid.

microorganisms to the initiation and progression of HCC still remains unclear.

The abundance of *Propionibacterium* significantly reduced in lung tumor tissues compared with that in nonmalignant adjacent tissues[13]. Another study suggested that *Propionibacterium* was responsible for a persistent, low-grade infection in the prostate, which triggered an inflammatory mechanism potentially contributing to the development of prostate cancer[14]. We detected statistically significant differences in the abundance and distribution of *Propionibacterium* between the HCC and peritumoral groups. *Propionibacterium* was more abundant in HCC tissues than in the adjacent tissues; however, its contribution to the initiation and progression of HCC remains unclear. The proliferation and migration of HUH-7 and HCC-LM3 cells decreased *in vitro* after coculture with *Propionibacterium* sp. and its supernatant. These findings suggest that *Propionibacterium* exerts its effects through specific metabolites.

Propionibacterium can anaerobically ferment lactose into PA[15]. A previous study demonstrated that PA induced cell death in cervical cancer cells[16]. We explored the effect of PA on HCC, for which the PA concentration was selected based on its effect on the proliferation capacity of HCC cells. The wound healing assay and Transwell experiments showed that the migration ability of HCC cells was inhibited at 10mM PA concentration.

The NF-κB signaling pathway is widely recognized as a crucial regulator of cell survival and tumor development, exerting antiapoptotic effects and promoting tumorigenesis[17]. The prevailing and extensively explored functions of NF-κB involve the activation of growth-promoting genes, such as c-myc and cyclin D1, as well as the stimulation of antiapoptotic genes, including c-IAP-1 and c-IAP-2[18]. In this study, *Propionibacterium* and PA exerted inhibitory effects on the NF-κB pathway.

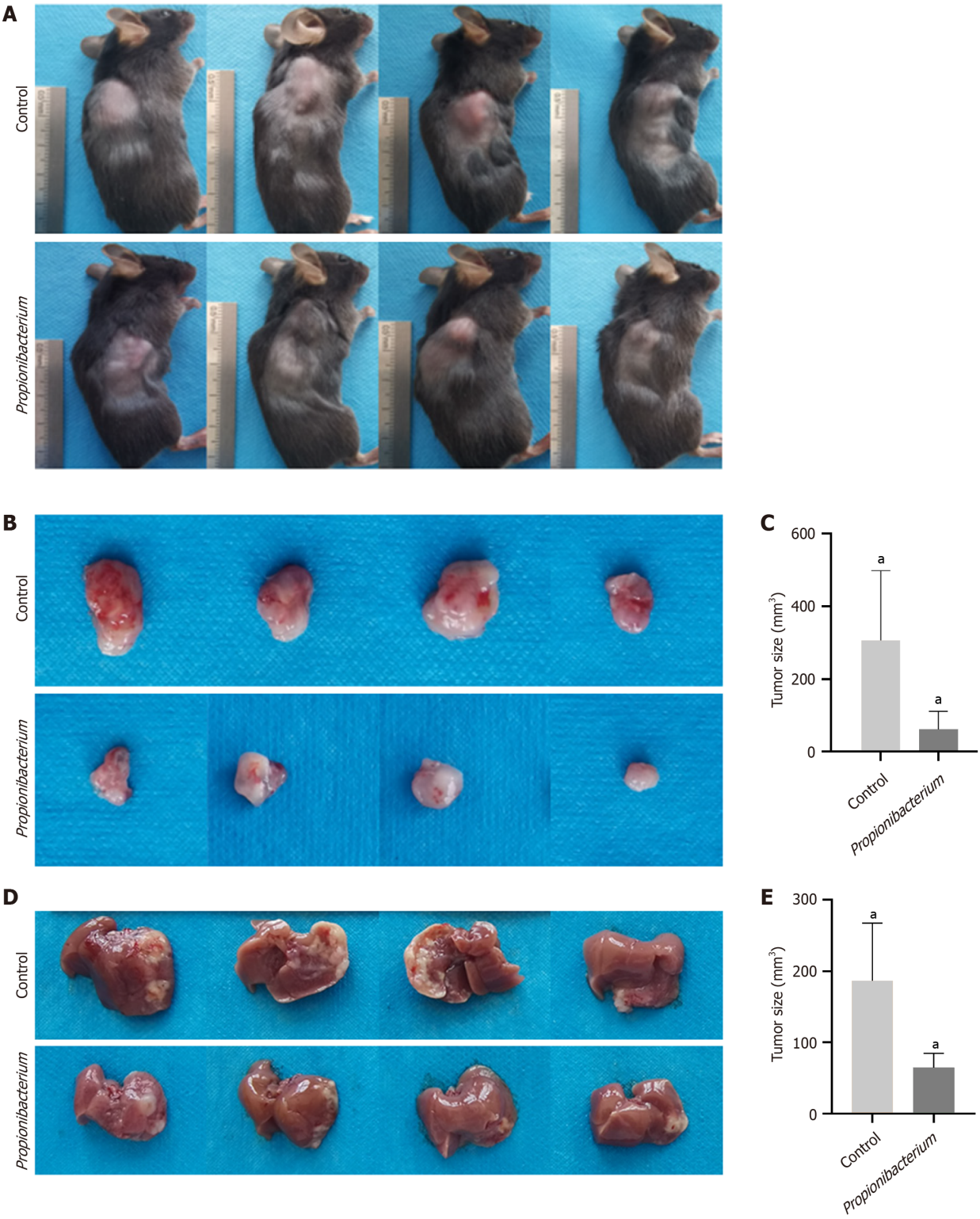

Figure 6 *Propionibacterium* and propionic acid repressed *in vivo* hepatocellular carcinoma tumorigenesis. A: Tumor formation in mice implanted with subcutaneous tumor after 2 weeks. The mice showed varying degrees of emaciation; B: Subcutaneous tumors after dissection; C: The subcutaneous tumor volume in control group was significantly higher than that in *Propionibacterium* group; D: Liver orthotopic implantation model was administered two weeks later; E: Tumor size of hepatocellular carcinoma in orthotopic model. $^{a}P < 0.05$.

To better simulate the process of HCC development in humans, we confirmed the role of *Propionibacterium* in tumor progression through subcutaneous implantation model and orthotopic liver transplantation model. The subcutaneous implantation model can be used to visually observe tumor growth. The conditions inside the liver are more complex than those inside the shallow fascia, and the improvement of cellular vitality plays a vital role in facilitating the successful establishment of implanted tumors[19,20]. We observed consistent results in both models, with significantly smaller tumors in the Propionibacterium group than in the control group. Furthermore, several mice were emaciated.

Our study had certain limitations. First, the timing of clinical specimen acquisition affected our findings, preventing us from monitoring the microbiota of patients with HCC in the early stages of HCC development. Changes in liver flora may be closely associated with oncogenesis. Second, this study was conducted at a single center, which may restrict the generalizability of the findings. Therefore, further experiments are required.

CONCLUSION

Overall, the microbiome of HCC tissues was characterized by 16S rRNA sequencing, and the effect of specific bacteria on the biological behavior of HCC cells was investigated.

FOOTNOTES

Author contributions: Cui ZL and Zheng B had full access to all of the data in the study and takes responsibility for the integrity of the data and the accuracy of the data analysis, they serve as co-corresponding authors of this paper; Liu BQ and Bai Y contributed equally to the experimental design, primary literature review, data extraction, data analysis, manuscript drafting and revision as co-first authors of this paper. Cui ZL, Zheng B and Liu BQ designed the research study; Liu BQ, Zheng B and Cui ZL performed the primary literature and data extraction; Liu BQ, Bai Y, Zhang YM, Wang TZ, Chen JR and Liu XY analyzed the data; Liu BQ, Zheng B and Cui ZL wrote the manuscript; Cui ZL, Zheng B, Bai Y and Liu BQ critically revised the manuscript for important intellectual content; and all authors read and approved the final version.

Supported by the Tianjin Health Science and Technology Project Surface Project, No. TJWJ2023MS012.

Institutional animal care and use committee statement: This study was reviewed and approved by Animal Ethics Committee of Tianjin First Central Hospital.

Conflict-of-interest statement: All the Authors have no conflict of interest related to the manuscript.

Data sharing statement: No additional data are available.

ARRIVE guidelines statement: The authors have read the STROBE Statement—checklist of items, and the manuscript was prepared and revised according to the STROBE Statement—checklist of items.

Country of origin: China

ORCID number: Zi-Lin Cui 0000-0002-0088-0322.

S-Editor: Lin C
L-Editor: A
P-Editor: Zhao S

REFERENCES

1 **Sung H**, Ferlay J, Siegel RL, Laversanne M, Soerjomataram I, Jemal A, Bray F. Global Cancer Statistics 2020: GLOBOCAN Estimates of Incidence and Mortality Worldwide for 36 Cancers in 185 Countries. *CA Cancer J Clin* 2021; **71**: 209-249 [PMID: 33538338 DOI: 10.3322/caac.21660]
2 **Toh MR**, Wong EYT, Wong SH, Ng AWT, Loo LH, Chow PK, Ngeow J. Global Epidemiology and Genetics of Hepatocellular Carcinoma. *Gastroenterology* 2023; **164**: 766-782 [PMID: 36738977 DOI: 10.1053/j.gastro.2023.01.033]
3 **Singal AG**, Lampertico P, Nahon P. Epidemiology and surveillance for hepatocellular carcinoma: New trends. *J Hepatol* 2020; **72**: 250-261 [PMID: 31954490 DOI: 10.1016/j.jhep.2019.08.025]
4 **Rumgay H**, Arnold M, Ferlay J, Lesi O, Cabasag CJ, Vignat J, Laversanne M, McGlynn KA, Soerjomataram I. Global burden of primary liver cancer in 2020 and predictions to 2040. *J Hepatol* 2022; **77**: 1598-1606 [PMID: 36208844 DOI: 10.1016/j.jhep.2022.08.021]
5 **El Tekle G**, Garrett WS. Bacteria in cancer initiation, promotion and progression. *Nat Rev Cancer* 2023; **23**: 600-618 [PMID: 37400581 DOI: 10.1038/s41568-023-00594-2]
6 **Poore GD**, Kopylova E, Zhu Q, Carpenter C, Fraraccio S, Wandro S, Kosciolek T, Janssen S, Metcalf J, Song SJ, Kanbar J, Miller-Montgomery S, Heaton R, Mckay R, Patel SP, Swafford AD, Knight R. Microbiome analyses of blood and tissues suggest cancer diagnostic approach. *Nature* 2020; **579**: 567-574 [PMID: 32214244 DOI: 10.1038/s41586-020-2095-1]
7 **He Y**, Zhang Q, Yu X, Zhang S, Guo W. Overview of microbial profiles in human hepatocellular carcinoma and adjacent nontumor tissues. *J Transl Med* 2023; **21**: 68 [PMID: 36732743 DOI: 10.1186/s12967-023-03938-6]

8 **Ghaddar B**, Biswas A, Harris C, Omary MB, Carpizo DR, Blaser MJ, De S. Tumor microbiome links cellular programs and immunity in pancreatic cancer. *Cancer Cell* 2022; **40**: 1240-1253.e5 [PMID: 36220074 DOI: 10.1016/j.ccell.2022.09.009]

9 **Ma Y**, Chen H, Li H, Zheng M, Zuo X, Wang W, Wang S, Lu Y, Wang J, Li Y, Wang J, Qiu M. Intratumor microbiome-derived butyrate promotes lung cancer metastasis. *Cell Rep Med* 2024; **5**: 101488 [PMID: 38565146 DOI: 10.1016/j.xcrm.2024.101488]

10 **Yu H**, Lin L, Zhang Z, Zhang H, Hu H. Targeting NF-κB pathway for the therapy of diseases: mechanism and clinical study. *Signal Transduct Target Ther* 2020; **5**: 209 [PMID: 32958760 DOI: 10.1038/s41392-020-00312-6]

11 **Israël A**. The IKK complex, a central regulator of NF-kappaB activation. *Cold Spring Harb Perspect Biol* 2010; **2**: a000158 [PMID: 20300203 DOI: 10.1101/cshperspect.a000158]

12 **Johnson JS**, Spakowicz DJ, Hong BY, Petersen LM, Demkowicz P, Chen L, Leopold SR, Hanson BM, Agresta HO, Gerstein M, Sodergren E, Weinstock GM. Evaluation of 16S rRNA gene sequencing for species and strain-level microbiome analysis. *Nat Commun* 2019; **10**: 5029 [PMID: 31695033 DOI: 10.1038/s41467-019-13036-1]

13 **Mao Q**, Ma W, Wang Z, Liang Y, Zhang T, Yang Y, Xia W, Jiang F, Hu J, Xu L. Differential flora in the microenvironment of lung tumor and paired adjacent normal tissues. *Carcinogenesis* 2020; **41**: 1094-1103 [PMID: 32658980 DOI: 10.1093/carcin/bgaa044]

14 **Shannon BA**, Garrett KL, Cohen RJ. Links between Propionibacterium acnes and prostate cancer. *Future Oncol* 2006; **2**: 225-232 [PMID: 16563091 DOI: 10.2217/14796694.2.2.225]

15 **Achermann Y**, Goldstein EJ, Coenye T, Shirtliff ME. Propionibacterium acnes: from commensal to opportunistic biofilm-associated implant pathogen. *Clin Microbiol Rev* 2014; **27**: 419-440 [PMID: 24982315 DOI: 10.1128/CMR.00092-13]

16 **Pham CH**, Lee JE, Yu J, Lee SH, Yu KR, Hong J, Cho N, Kim S, Kang D, Lee S, Yoo HM. Anticancer Effects of Propionic Acid Inducing Cell Death in Cervical Cancer Cells. *Molecules* 2021; **26** [PMID: 34443546 DOI: 10.3390/molecules26164951]

17 **Tabruyn SP**, Griffioen AW. NF-kappa B: a new player in angiostatic therapy. *Angiogenesis* 2008; **11**: 101-106 [PMID: 18283548 DOI: 10.1007/s10456-008-9094-4]

18 **Dolcet X**, Llobet D, Pallares J, Matias-Guiu X. NF-kB in development and progression of human cancer. *Virchows Arch* 2005; **446**: 475-482 [PMID: 15856292 DOI: 10.1007/s00428-005-1264-9]

19 **Reiberger T**, Chen Y, Ramjiawan RR, Hato T, Fan C, Samuel R, Roberge S, Huang P, Lauwers GY, Zhu AX, Bardeesy N, Jain RK, Duda DG. An orthotopic mouse model of hepatocellular carcinoma with underlying liver cirrhosis. *Nat Protoc* 2015; **10**: 1264-1274 [PMID: 26203823 DOI: 10.1038/nprot.2015.080]

20 **Cheung PF**, Yip CW, Ng LW, Lo KW, Wong N, Choy KW, Chow C, Chan KF, Cheung TT, Poon RT, Fan ST, Cheung ST. Establishment and characterization of a novel primary hepatocellular carcinoma cell line with metastatic ability in vivo. *Cancer Cell Int* 2014; **14**: 103 [PMID: 25349534 DOI: 10.1186/s12935-014-0103-y]

Published by **Baishideng Publishing Group Inc**
7041 Koll Center Parkway, Suite 160, Pleasanton, CA 94566, USA
Telephone: +1-925-3991568
E-mail: office@baishideng.com
Help Desk: https://www.f6publishing.com/helpdesk
https://www.wjgnet.com